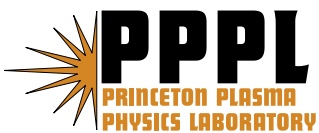


**3D Modeling of the Sawtooth Instability
in a Small Tokamak**

J.A. Breslau, S.C. Jardin, and W. Park

Preprint
(February 2007)



Princeton Plasma Physics Laboratory

Report Disclaimers

Full Legal Disclaimer

This report was prepared as an account of work sponsored by an agency of the United States Government. Neither the United States Government nor any agency thereof, nor any of their employees, nor any of their contractors, subcontractors or their employees, makes any warranty, express or implied, or assumes any legal liability or responsibility for the accuracy, completeness, or any third party's use or the results of such use of any information, apparatus, product, or process disclosed, or represents that its use would not infringe privately owned rights. Reference herein to any specific commercial product, process, or service by trade name, trademark, manufacturer, or otherwise, does not necessarily constitute or imply its endorsement, recommendation, or favoring by the United States Government or any agency thereof or its contractors or subcontractors. The views and opinions of authors expressed herein do not necessarily state or reflect those of the United States Government or any agency thereof.

Trademark Disclaimer

Reference herein to any specific commercial product, process, or service by trade name, trademark, manufacturer, or otherwise, does not necessarily constitute or imply its endorsement, recommendation, or favoring by the United States Government or any agency thereof or its contractors or subcontractors.

PPPL Report Availability

Princeton Plasma Physics Laboratory:

<http://www.pppl.gov/techreports.cfm>

Office of Scientific and Technical Information (OSTI):

<http://www.osti.gov/bridge>

Related Links:

[U.S. Department of Energy](#)

[Office of Scientific and Technical Information](#)

[Fusion Links](#)

3D modeling of the sawtooth instability in a small tokamak

J.A. Breslau, S.C. Jardin, W. Park

Plasma Physics Laboratory, Princeton University, P.O. Box 451, Princeton, NJ 08543,
USA and SciDAC Center for Extended MHD Modeling (CEMM)

E-mail: jbreslau@pppl.gov

Abstract. The sawtooth instability is one of the most fundamental dynamics of an inductive tokamak discharge such as will occur in the International Thermonuclear Experimental Reactor (ITER) [R. Aymar *et al.*, Plasma Phys. Controlled Fusion **44**, 519 (2002)]. Sawtooth behavior is complex and remains incompletely explained. The Center for Extended MHD Modeling (CEMM) SciDAC project has undertaken an ambitious campaign to model this periodic motion in a small tokamak as accurately as possible using the Extended MHD model. Both M3D [W. Park, *et al.*, Phys. Plasmas **6**, 1796 (1999)] and NIMROD [C.R. Sovinec *et al.*, Phys. Plasmas **10**, 1727 (2003)] have been applied to this problem. Preliminary nonlinear MHD results show pronounced stochasticity in the magnetic field following the sawtooth crash but are not yet fully converged. Compared to the MHD model, Extended MHD predicts plasma rotation, faster reconnection, and reduced field line stochasticity in the crash aftermath. The multiple time and space scales associated with the reconnection layer and growth time make this an extremely challenging computational problem. However, these calculations are providing useful guidelines to the numerical and physical requirements for more rigorous future studies.

I. Introduction

The sawtooth crash is an internal MHD reconnection event which repeatedly mixes plasma from the core and outer regions of tokamaks, cooling and flattening the central temperature profile¹. Occurring in discharges in which the tendency for the toroidal current to peak drives the central safety factor q below unity, the crash has the character of an internal kink mode, with dominant poloidal and toroidal mode numbers $m=n=1$. The standard picture of the event² has the hot core region within the $q=1$ surface undergoing magnetic reconnection along a helical X-line to be replaced by a cold, 1,1 island. Many measurements have called details of this model into question, however³, and the precise triggering mechanism and long-term dynamics of the crash are still not well understood. It is desirable to develop a model of such events that provides a quantitative predictive capability so that they can be avoided or controlled. Analytic theories and quasi-empirical theory-based models such as that of Porcelli⁴ provide a good starting point, but more fundamental numerical models stand a better chance of giving precise and accurate predictions of sawtooth thresholds and periods for particular discharges in particular physical devices and for testing and optimizing various control techniques.

The M3D (Multilevel 3D)⁵ and NIMROD⁶ codes were designed for the study of such macroscopic instabilities. The workhorse codes of the SciDAC Center for Extended MHD Modeling, they can employ any of a hierarchy of fluid and fluid-particle hybrid models in tracking the nonlinear evolution of magnetically confined plasmas in three dimensions. Both employ finite element methods on series of 2D planes in cylindrical coordinates R and Z , but they differ in the orders of those elements, the structure of their meshes, and in whether the toroidal direction is resolved in real or Fourier space. The M3D code uses a partially implicit time integration algorithm in which the fast wave and diffusive terms are treated implicitly but the shear Alfvén, slow wave, and convective terms are all explicit; the NIMROD code is more fully implicit, particularly in the linear regime. Both codes are capable of linear operation (predicting eigenmodes and their growth rates) as well as nonlinear time advancing.

For the study described here, both the resistive MHD model and a more complete Extended MHD model were used.

It is well-known that resistive MHD phenomena involving magnetic reconnection, such as the sawtooth crash, are associated with thin sheets of high current density whose thickness scales as $S^{-1/2}$, where the Lundquist number S is the ratio of the resistive diffusion time to the Alfvén transit time in the plasma. Because S is proportional to the system size and the temperature to the 3/2 power, $S \propto aT^{3/2}$, its value in present-day large tokamak experiments is large, typically of the order of 10^8 or higher, which implies severe resolution requirements that are not practical for today’s codes and computers. Such high-temperature discharges also require a more complete kinetic model than is presently available. Modeling sawteeth in large tokamaks involves a large disparity in time scales as well: one needs to resolve in one simulation both the detailed dynamics of a crash (occurring on the order of $10 \mu\text{s}$) and of the heating period between the crashes (taking on the order of seconds for ITER), preferably for several cycles, while (in the explicit code) taking steps on the order of the shear Alfvén transit time for a single mesh zone, on the order of ns, necessitating a prohibitively large number of time steps. In contrast, smaller, colder tokamaks with S of 10^5 or lower have less extreme current sheets that can be adequately resolved in a long calculation, and have much shorter crash and cycle times, and so are better candidates for realistic MHD physics simulation on present-day computers. The resistive MHD model gives a reasonable description of magnetic reconnection in these devices, although there are some quantitative differences when the more complete extended MHD model is used.

The Current Drive Experiment Upgrade (CDX-U)⁷ is a small ($R_0=33.5 \text{ cm}$), low-aspect-ratio university-scale tokamak at the Princeton Plasma Physics Laboratory. Its discharges are much colder ($T_e \sim 100 \text{ eV}$) and briefer (on the order of a few ms) than those in larger experiments, but it is reasonably well-diagnosed, and exhibits the same MHD instabilities that are of interest in reactor-relevant devices, including a sawtooth regime with a period of approximately $500 \mu\text{s}$. With $S \approx 10^4$, it is

an ideal testbed for modeling with present-day extended MHD codes and for comparing their predictions in the far nonlinear regime.

This paper describes a preliminary set of tests in which the M3D and NIMROD codes were applied to a test problem consisting of a simplified model of a typical CDX-U discharge in an effort to reproduce basic sawtooth behavior, compare the behavior of the two codes in the nonlinear regime, and determine the requirements for a more detailed study. In Section II, we set out the choices of physical parameters and details of the numerical model for the CDX-U sawtooth simulation. In Section III, results of a linear MHD study are presented. Section IV describes the results of the nonlinear MHD study with M3D, including attempts at convergence in mesh resolution. Section V shows the effects of two-fluid terms on the nonlinear behavior. Section VI contains our conclusions.

II. Statement of the problem

Our goal for this preliminary study was not to precisely reproduce the signals observed in a particular sawtooth discharge in CDX-U, but rather to attempt to model the general characteristics of such discharges to assess the resolution and model requirements and general feasibility of such a study. Our priorities were to construct a relatively simple, clean, well-defined problem that could be run by both M3D and NIMROD for comparison in the nonlinear regime, and to determine which physics was most essential for accurately capturing sawtooth behavior. Accordingly, we do not show experimental data in this article; the interested reader may, however, refer to the article by Kaita, *et al.* in this issue for typical diagnostic traces from MHD activity in CDX-U.

The numerical study begins with a sequence of equilibria that occur as time slices from a reconstruction of a typical CDX-U discharge using the axisymmetric time-dependent free-boundary transport timescale code TSC⁸ to closely match the characteristics of the actual experiment. Using an internal feedback system, we programmed the currents in the OH coils so that we match a typical time-trace⁹ of the plasma current that ramps up from 5 to ~50 kA in 5-6 ms with a waveform that corresponds to two capacitor banks being discharged. The PF coil currents are pre-programmed to

match the experimental values, with an additional feedback system to keep the plasma centered in the vessel as is done experimentally. A density profile was prescribed to be linear in the poloidal flux variable, and increasing in time to match the measured line average density, which peaked at about $8 \times 10^{18} \text{ m}^{-3}$. The standard TSC transport model¹⁰ was used with a coefficient adjusted to approximately match the central electron temperature vs. time, which peaked at about 80 eV. The overall energy confinement time corresponding to this came out to be about 150 μs , corresponding to about 200 kW (peak) of Ohmic heating power and 30 J of stored energy. The actual χ_e profile used ranged from about 20 m^2/s in the center to 2000 m^2/s at the edge. The central safety factor, q_0 , begins at around 10 and drops during the discharge, passing through 1 between 5 and 6 ms. The sawtooth model in TSC is turned off, and so we write equilibrium files periodically after q_0 passes through one for subsequent analysis by the M3D code.

The reference case for the simulations described in the rest of this paper is one for which q_0 has dropped to 0.92, increasing monotonically outward, with the $q=1$ surface approximately one-third of the way out from the axis. This somewhat arbitrary choice was made simply to ensure the existence of an MHD-unstable $n=1$ mode, and represents a compromise between lower- q_0 equilibria, which have similar unstable modes with higher linear growth rates; and higher- q_0 equilibria which may be more faithful to the actual physical device but which are at best marginally unstable. While the first simulated crash arising from the $q_0=0.92$ case may not closely resemble the triggering mechanism in the device, subsequent crashes during the same run are expected to model it more self-consistently.

The magnetic field and the pressure and density profiles are read into M3D from the equilibrium file and used to initialize both the fixed-boundary geometry (with a flux-surface-aligned unstructured triangular mesh) and the fields themselves. The initial resistivity is taken to be the Spitzer value based on the initial temperature profile, which gives a peak S of 1.94×10^4 , with the minimum value constrained to be no smaller than 1.94×10^2 . The resistivity is not evolved in time. The viscosity is set to ten times the resistivity at the peak location and is constant in space and time. The unstructured mesh used 79 zones in the radial direction, giving it a resolution of approximately 9200 vertices in

each poloidal cross-section. Because the initial equilibrium is axisymmetric, linear modes with different toroidal mode number n decouple, although each contains a wide range of poloidal modes $0 \leq m \leq m_{max}$ represented on the finite element grid.

The first objective was to run the code in its linear mode in order to determine the eigenmodes and linear growth rates of the starting equilibrium for the first few toroidal mode numbers, $n=1-7$. The dependencies of these modes and growth rates on the choice of transport coefficients were also investigated. The primary studies are full nonlinear runs of the code, initialized by superimposing the $n=1$ eigenmode found in the previous study on the equilibrium state at an amplitude such that the maximum B_p in the perturbation is 10^{-4} of the maximum B_T in the equilibrium. The plasma is allowed to evolve in the presence of volumetric source terms chosen to restore the current density and temperature to their equilibrium values. The two highest- n resolvable toroidal modes are filtered out to avoid aliasing problems; the others are kept and couple to each other in a fully nonlinear way. The behavior of the current and temperature profiles and of the field topology are closely monitored for indications of $m=1$ activity as the equations are solved out to several predicted sawtooth periods. The study is then repeated with an Extended MHD model by including the ion diamagnetic (ω_i^*) term¹¹ in the momentum equation to model the effects of ion gyroviscosity.

III. Linear MHD results

The linear search for an unstable $n=1$ eigenmode of the provided equilibrium revealed that such a mode does exist (figure 1a). It has a predominantly $m=1$ character contained within the $q=1$ rational surface, consistent with the sawtooth model, and a normalized linear growth rate in the absence of thermal conduction of $\gamma\tau_A \approx 8.61 \times 10^{-3}$.

A search for unstable higher- n modes also yielded positive results. As shown in figures 1b,c, they tend to occur near the boundary. These modes have growth rates higher than that of the $n=1$ mode, said rates increasing with n and approximately in proportion to $n^{3/5}$. This scaling and the location of the modes both suggest that these should be identified as resistive ballooning modes¹². Their growth rates

are reduced by the addition of a realistic level of parallel heat conduction, but can be linearly stabilized only by the additional imposition of a large perpendicular heat conduction: approximately $200 \text{ m}^2/\text{s}$, consistent with the boundary value required in the TSC reconstruction to reproduce the temperature profiles observed in the experiment. We conjecture that the self-consistent thermal transport associated with these modes may account for the anomalously high value of the heat conduction¹³, thereby acting as a nonlinear feedback mechanism to stabilize them at a small amplitude in the experiment.

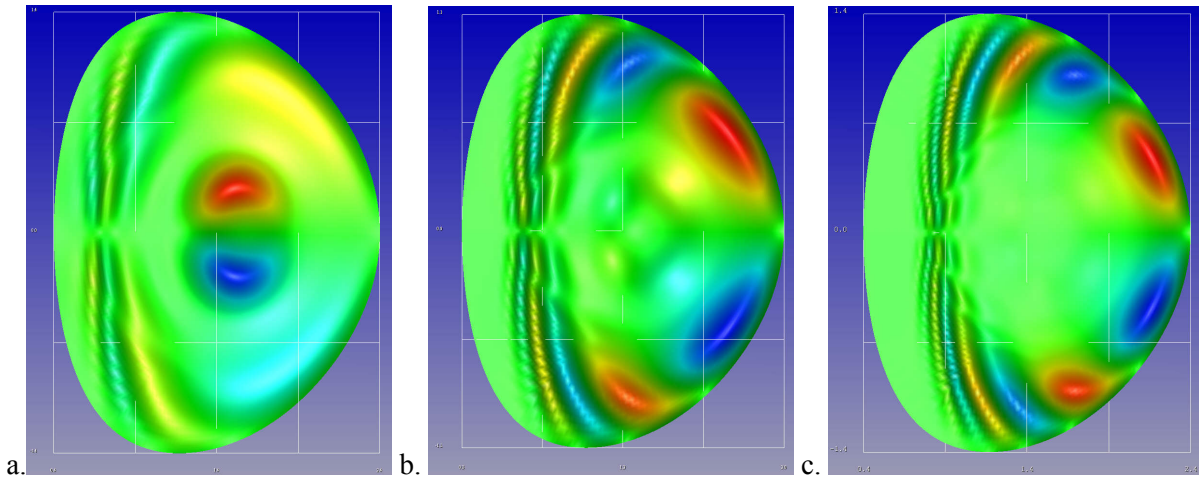


Figure 1: a. Velocity stream functions in the $\phi=0$ plane for eigenmodes of the $q=0.92$ CDX equilibrium found by the M3D code. a. $n=1$ mode, showing primarily $m=1$ character. b. $n=2$ mode. c. $n=3$ mode.

Following the discovery of the need for this high perpendicular heat conduction, the calculation of the $n=1$ mode was repeated. The artificial sound implementation of parallel heat conduction was switched on in M3D as well, with an effective electron thermal speed of $6 v_A$, consistent with the experiment. The presence of heat conduction was found not to significantly change the shape of the eigenmode, but did have a stabilizing effect, reducing its projected growth rate to $\gamma\tau_A \approx 5.1 \times 10^{-3}$. This growth rate and eigenmode are in good agreement with the NIMROD prediction at these parameters.

IV. Nonlinear MHD results

A. Sawtooth cycle

To initialize the nonlinear study with M3D, the $n=1$ eigenmode described in section III was added as a small initial perturbation to the unstable equilibrium. Both parallel and perpendicular heat conduction were employed as described above, stabilizing the higher- n modes. As shown in figure 2a, this nonlinear run begins with a long phase of essentially linear behavior during which the $n=1$ mode grows at the linearly predicted rate, while nonlinearly coupling to and destabilizing higher n modes. These higher- n modes have predominantly $m=n$ character and are at the $q=1$ surface, and so should not be confused with the higher- n eigenmodes seen near the boundary in the linear study.

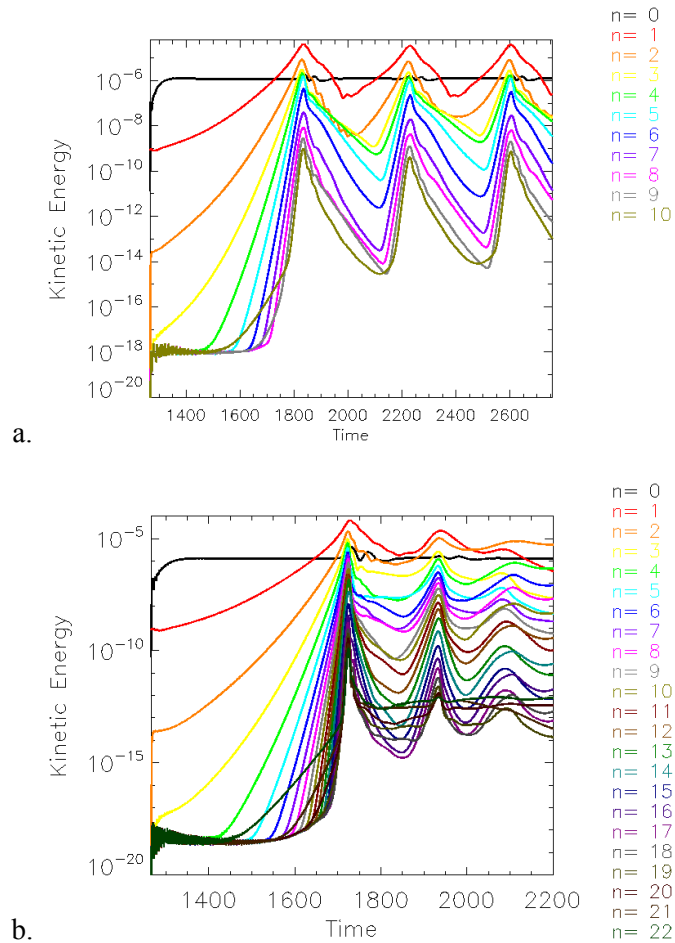


Figure 2: Total kinetic energy (arbitrary units) on a logarithmic scale by mode number during M3D

nonlinear sawtooth runs at moderate and high toroidal resolutions. Three sawtooth crashes (associated with peaks in energy) are shown. Times are in Alfvén times. **a.** 10 toroidal modes retained. **b.** 22 modes retained.

The sequence of Poincaré plots in figure 3 shows the evolution of the magnetic flux surfaces during a typical sawtooth cycle. The nonlinear $m=1$, $n=1$ mode results in a complete sawtooth crash, with formation of a new magnetic axis, and reconnection of the original one, as in the Kadomtsev model². The high-temperature region associated with the original axis is mixed with the outer plasma, and replaced by the flat-temperature 1,1-island, producing the temperature drop diagnostic of the sawtooth (figure 4). Because the $n=1$ mode and the nonlinearly driven higher- n modes also have higher m components at rational surfaces with $q>1$, the (1,1) island merging coincides with the growth and overlap of other island chains at larger minor radii, resulting in general stochasticity after the “crash”. This stochasticity does not, as one might expect, flatten the temperature profile in the outer region; the finite size of the parallel thermal conductivity in the model is insufficient to completely equalize temperature along the long stochastic field lines before the surfaces have time to heal. As the current source term gradually drives the central safety factor back below unity, and the temperature source reheats the cooled core region, the stochastic regions heal and again become good flux surfaces. The process then repeats. The cycle time of $395 \tau_A$ is equivalent to about $100 \mu\text{s}$, substantially shorter than the typical experimental value for reasons to be discussed in the final section.

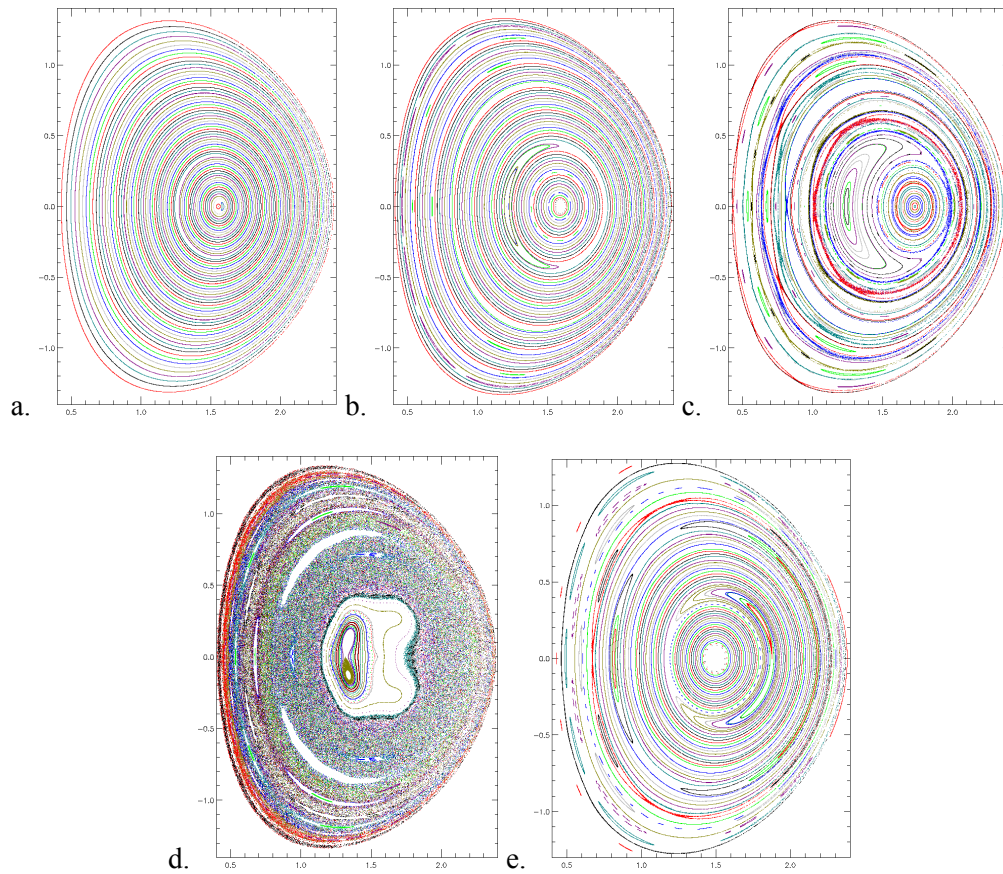


Figure 3: Poincaré sections showing intersection of magnetic surfaces with the $\phi=0$ plane at several time slices during the course of the nonlinear 10-mode CDX run depicted in figure 3. **a.** Initial state, $t=1266.17$. **b.** Island growing, $t=1660.70$. **c.** Nonlinear phase, $t=1795.61$. **d.** After first crash, $t=1839.86$. **e.** Flux surfaces recovered, $t=2094.08$.

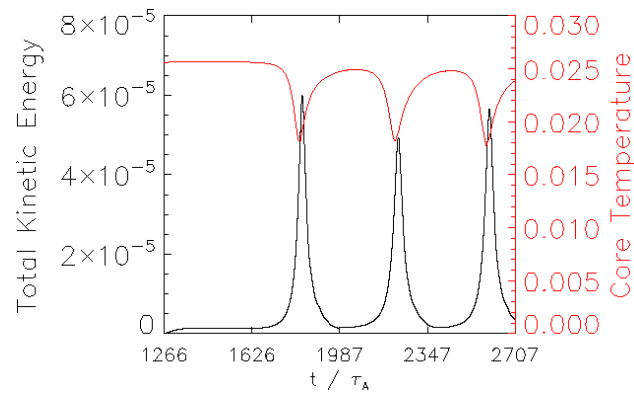


Figure 4: Total kinetic energy (black curve) and core temperature (red curve) vs. time during the 10-mode nonlinear CDX sawtooth run with M3D, illustrating temperature crashes and recoveries.

B. Convergence study

In order to assess numerical convergence, the nonlinear study was repeated with the same poloidal resolution but with twice the toroidal resolution, allowing modes up to $n=22$ to be resolved. The behavior of the higher-resolution run, however, was significantly different from that of the initial one. The initial crash happened sooner and with greater violence, and subsequent crashes followed with a shorter period but with diminishing energy (figure 2b). This failure to converge with more planes appears to be caused by the presence of large amounts of energy in the additional modes. We are performing additional studies to determine whether these short-wavelength modes are physical or are artifacts of converging in only one dimension or of the simplified resistive MHD model.

V. Extended MHD Results

In order to determine to lowest order the effects of physics beyond the resistive MHD model on the sawtooth under investigation, the ten-mode nonlinear run described above was repeated with the ion diamagnetic terms in the M3D code switched on. The same MHD $n=1$ eigenmode was used for the initial perturbation. The strength of the added term is characterized by a dimensionless parameter equivalent to the ratio of the collisionless ion skin depth to the length scale of the system (the minor radius). For this study, the parameter was taken to be 0.05, which is its approximate value in the experiment.

Figure 5 illustrates the nonlinear behavior of the kinetic energy during the course of a two-fluid sawtooth cycle. It is evidently similar to the resistive MHD case, but with some qualitative distinguishing features. Most notable are the oscillations in the energies of the higher n modes as they couple to the $n=1$ mode and to each other and grow in the period preceding the first crash. These appear to be associated with the differential rotation induced by the presence of the diamagnetic term. A secondary observation is that the sawtooth period has lengthened somewhat in comparison to the MHD result at the same toroidal resolution – to $406.7 \tau_A$, up from 395.

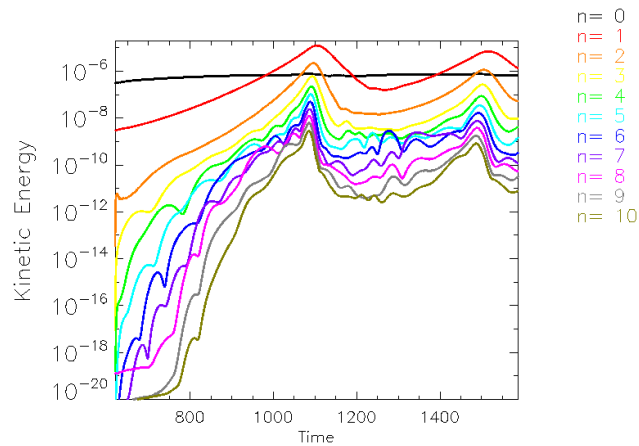


Figure 5: Kinetic energy (arbitrary units) by mode number during two-fluid nonlinear sawtooth run. Times are in Alfvén times. 10 toroidal modes retained.

Other effects of including the extra term can be seen in the series of Poincaré plots in figure 5. The most noticeable difference in comparison with figure 3 is the expected rotation of the 1,1 island about the magnetic axis. More striking is the absence of significant stochasticity following either crash. The rotation is evidently sufficient to damp growth of the outer islands, leaving good surfaces following the crash as expected in the experiment; this is an indication of the importance of adding the term for capturing the correct physics. Finally, reconnection is observed to be incomplete in the second crash. Whether this represents a real consequence of two-fluid physics or is a side effect of the lesser energy of the second crash remains to be determined in convergence studies to follow.

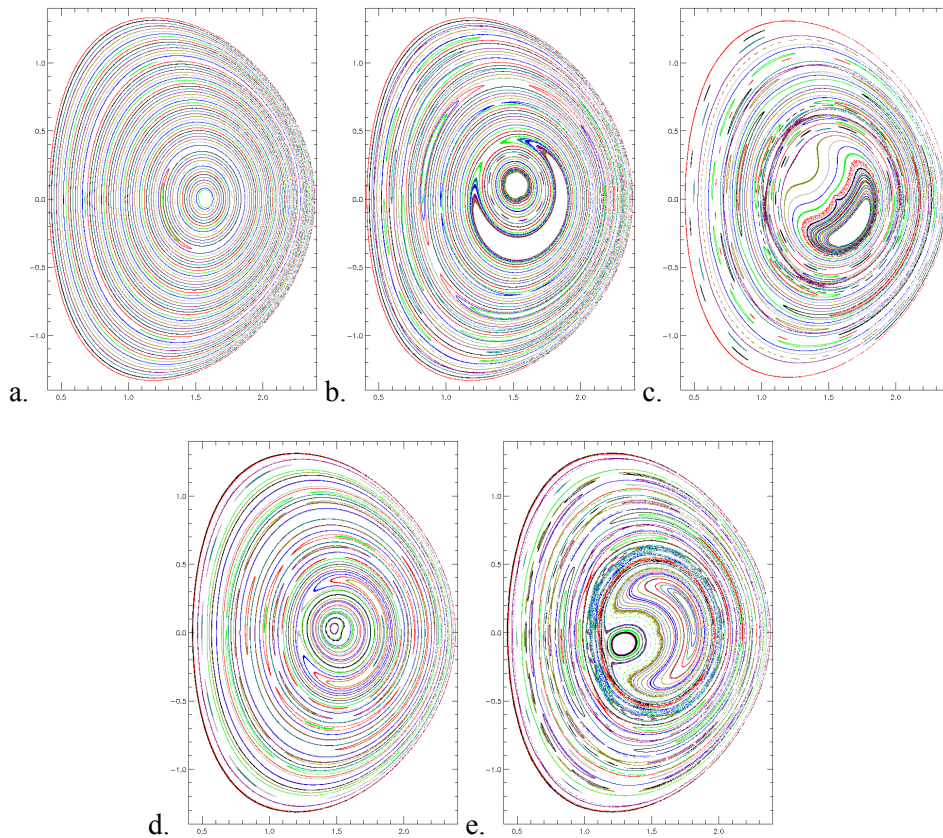


Figure 5: Poincaré sections showing intersection of magnetic surfaces with the $\phi=0$ plane at several time slices during the course of the nonlinear two-fluid 10-mode CDX run depicted in figure 5. **a.** Early state, $t=653.95$. **b.** Nonlinear phase, $t=1008.38$. **c.** After first crash, $t=1118.44$. **d.** Between crashes, $t=1316.83$. **e.** After second crash, $t=1502.53$.

VI. Summary and Discussion

In a series of high-resolution, massively parallel nonlinear MHD runs totaling approximately 100,000 CPU-hours, the sawtooth cycle in the CDX tokamak has been tracked with the M3D code. This preliminary study revealed the existence of unstable resistive ballooning modes in the equilibrium, which are stabilized by the presence of a large perpendicular heat conduction in what may be an example of nonlinear saturation of the modes. Good agreement was seen between the M3D and NIMROD predictions of the linear $n=1$ mode. The nonlinear run exhibited a series of repeating

sawtooth crashes, though with a cycle time significantly less than that seen in the experiment. In the MHD case, the crashes are associated with a general stochasticization of the magnetic field throughout the plasma, but this stochasticity does not significantly flatten the temperature profile outside the $q=1$ surface and is short-lived, quickly healing back to good flux surfaces after each crash. Although the sawtooth is predominantly a low-toroidal and -poloidal-mode-number event, the nonlinear resistive MHD study failed to converge as the toroidal resolution was increased. The nonlinear two-fluid results included rotation of the plasma, a sawtooth period slightly closer to that of the experiment, and a lack of widespread stochasticity following the crash. Tests for agreement of the nonlinear results with those of the NIMROD code are left to a future study.

The lessons learned from this study make it possible to more clearly define what is needed to set up a more physically meaningful test problem. Important physical effects are captured only by the two-fluid model, so this will be required for follow-up work. The sensitivity of the sawtooth period to the sources and the transport model indicates that these will have to show greater fidelity to the experimental profiles if we hope to accurately reproduce the observations from the device. In particular, the use of ohmic heating and inductive current drive will be required, rather than the volume source terms now in use for these quantities, which do not have direct analogues in the device. A self-consistent evolving resistivity profile and a perpendicular heat transport profile with much smaller interior values will also be needed. In order to assess convergence, higher resolutions than the present study, both toroidally and poloidally, must be employed as well.

The task of scaling such studies up to ITER-scale devices remains a formidable challenge. The vastly higher temperatures and, to a lesser extent, the much larger physical size, will necessitate an increase of several orders of magnitude in spatial resolution, which, due to the partially explicit nature of the code, will also require orders of magnitude more time steps to reach the same physical time. In order to achieve this, we will not be able to rely solely on increases in hardware capability, but must also improve the software, making use of techniques such as adaptive mesh refinement and making the codes more efficient, more scalable, and more implicit.

Acknowledgments

The authors are grateful for useful discussions with R. Kaita, R. Majeski, and D. Stutman of the CDX-U team and with members of the SciDAC Center for Extended MHD Modeling (CEMM). We have benefited from numerous discussions with and from M3D code improvements made by H. Strauss, L. Sugiyama, G. Y. Fu, and J. Chen. The authors are indebted to members of the NIMROD team for many discussions and for making their simulation results freely available. In particular, we acknowledge D. Schnack, A. Pankin, S. Kruger, and C. Sovinec. We are also grateful for visualization support from S. Klasky. This work was supported by U.S. Department of Energy Contract No. DE-AC02-76CH03073 and by the Department of Energy SciDAC Center for Extended Magnetohydrodynamic Modeling. Calculations were performed at the National Energy Research Scientific Computing Center (NERSC) and at the National Center for Computational Sciences (NCCS) at the Oak Ridge National Laboratory.

References

- ¹S. von Goeler, W. Stodiek, and N. Sauthoff, *Phys. Rev. Lett.* **33**, 1201 (1974).
- ²B.B. Kadomtsev, *Sov. J. Plasma Phys.* **1**, 389 (1975).
- ³R.J. Hastie, *Astrophys. Space Sci.* **256**, 177 (1997).
- ⁴F. Porcelli, D. Boucher, and M. Rosenbluth, *Plasma Phys. Controlled Fusion* **38**, 2163 (1996).
- ⁵W. Park, E.V. Belova, G.Y. Fu, X.Z. Tang, H.R. Strauss, and L.E. Sugiyama, *Phys. Plasmas* **6**, 1796 (1999).
- ⁶C.R. Sovinec, T.A. Gianakon, E.D. Held, S.E. Kruger, and D.D. Schnack, *Phys. Plasmas* **10**, 1727 (2003).
- ⁷J. Menard, R. Majeski, R. Kaita, et al., *Phys. Plasmas* **6** 2002 (1999).
- ⁸S. Jardin, N. Pomphrey, and J.L. DeLucia, *J. Comp. Phys.* **66** 481 (1986).
- ⁹J. Menard, PhD Thesis, Princeton University (1998).
- ¹⁰S.C. Jardin, M.G. Bell, and N. Pomphrey, *Nucl. Fusion* **33** 371 (1993).
- ¹¹L.E. Sugiyama and W. Park, *Phys. Plasmas* **7** 4644 (2000).
- ¹²H.R. Strauss, *Phys. Fluids* **24**, 2004 (1981).
- ¹³B.A. Carreras and P.H. Diamond, *Phys. Fluids B* **1** 1011 (1989).

The Princeton Plasma Physics Laboratory is operated
by Princeton University under contract
with the U.S. Department of Energy.

Information Services
Princeton Plasma Physics Laboratory
P.O. Box 451
Princeton, NJ 08543

Phone: 609-243-2750
Fax: 609-243-2751
e-mail: pppl_info@pppl.gov
Internet Address: <http://www.pppl.gov>